


Novel single-chain variant of antibody against mesothelin established by phage library

Hiromasa Yakushiji^{1,2} | Kazuko Kobayashi^{1,3} | Fumiaki Takenaka³ | Yoshiro Kishi⁴ |
Midori Shinohara⁴ | Masaru Akehi³ | Takanori Sasaki³ | Eiji Ohno⁵ |
Eiji Matsuura^{1,3,6} 

¹Department of Cell Chemistry, Okayama University Graduate School of Medicine, Dentistry, and Pharmaceutical Sciences, Okayama, Japan

²Department of Medical Life Science Faculty of Medical Bioscience Kyushu, University of Health and Welfare, Miyazaki, Japan

³Collaborative Research Center for OMIC, Okayama University Graduate School of Medicine, Dentistry, and Pharmaceutical Sciences, Okayama, Japan

⁴Department of Research and Development, Ina Institute, Medical & Biological Laboratories, Co., Ltd, Ina, Japan

⁵Department of Medical Technology and Sciences, Faculty of Health Sciences, Kyoto Tachibana University, Kyoto, Japan

⁶Neutron Therapy Research Center, Okayama University, Okayama, Japan

Correspondence

Eiji Matsuura, Neutron Therapy Research Center, Okayama University, Okayama, Japan.

Email: ejimatu@md.okayama-u.ac.jp

Funding information

Japan Agency for Medical Research and Development

Abstract

Mesothelin (MSLN) shows increased expression in various cancer cells. For clinical application of antibodies as a positron emission tomography (PET) imaging reagent, a human shortened antibody is essential both for avoiding redundant immune responses and for providing rapid imaging. Therefore, we cloned a single-chain fragment of variable regions (scFv) from a human-derived gene sequence. This was achieved through the construction of a naïve phage library derived from human tonsil lymphocytes. Using a column with human recombinant MSLN, we carried out biopanning of phage-variants by colony formation. We first obtained 120 clones that were subjected to selection in an ELISA using human recombinant MSLN as a solid phase antigen, and 15 phage clones of scFv with a different sequence were selected and investigated by flow cytometry (FCM). Then, six variants were selected and the individual scFv gene was synthesized in the V_L and V_H domains and expressed in Chinese hamster ovary cells. Mammalian cell-derived human-origin scFv clones were analyzed by FCM again, and one MSLN highly specific scFv clone was established. PET imaging by ⁸⁹Zr-labeled scFv was done in mice bearing xenografts with MSLN-expressing cancer cells, and tumor legions were successfully visualized. The scFv variant established in the present study may be potentially useful for cancer diagnosis by PET imaging.

KEYWORDS

⁸⁹Zr (zirconium-89), mesothelin, phage library, positron emission tomography (PET) imaging, single-chain fragment of variable region

1 | INTRODUCTION

Mesothelin (MSLN) is a cell differentiation-related and cell surface glycoprotein (40 kDa) that includes a glycosylphosphatidylinositol (GPI) anchor.¹ In normal tissues, MSLN is expressed only in mesothelial cells in the pleura, peritoneum, and pericardium. However, in malignant tumors, MSLN is overexpressed in diverse types of cancers, such as ovarian cancer, gastric cancer, non-small cell lung cancer, breast cancer, pancreatic cancer, and malignant mesothelioma.²⁻¹³ MSLN and its variant, soluble MSLN-related peptide (SMRP), are possible biomarkers for malignant tumors. Commercially available ELISA to diagnose malignant mesothelioma based on recognition of SMRP are available.¹⁴⁻²² A clinical trial of anti-MSLN mAb, amatuximab (MORAb-009), for the treatment of mesothelioma and pancreatic cancer is now underway.

Monoclonal antibodies have been applied as powerful clinical tools for diagnosis (for cancer imaging) and treatment.²³⁻²⁵ However, full-length IgG has a long circulation time in the blood and undesirable characteristics, such as accumulation in the liver. In contrast, small-sized antibody variants, such as single-chain fragment of variable region (scFv), diabody, minibody, and F(ab')₂ can penetrate tumors and other tissues faster and more uniformly than full-length IgG.²⁶⁻³⁰ A deletion of Fc domain allows evasion of immune detection. As a result, in vivo clearance of specific antibody is accelerated, and nonspecific accumulation is expected to be reduced. Furthermore, with these effects, highly specific imaging can be achieved in a shortened imaging period. Specificity to antigen in the molecule, ease of preparation by gene recombination, and high permeability to tumors because of its small molecular size make scFv an extremely attractive reagent. Nevertheless, PET imaging with scFv is presently rare other than in some cases of ovarian cancer.³¹

In our previous PET imaging study, MSLN-positive tumors in xenografts were visibly detected by ⁶⁴Cu-radiolabeled full-length mouse antihuman MSLN IgG, but it took 24-48 hours to get fine contrast as a result of the long half-life of IgG.³² In the present study, we established a scFv from a human-origin gene sequence and rapid PET imaging (3 hours after the injection) of tumor regions was successfully demonstrated in xenografts using the scFv.

2 | MATERIALS AND METHODS

2.1 | Reagents

Deferoxamine-*p*-SCN (DFO) was purchased from Macrocyclics. Amicon Ultra 0.5 centrifugal filter units were purchased from Merck Millipore. Other chemicals were reagent grade.

2.2 | Construction of phage antibody library

Phage antibody library was constructed by using human tonsils removed from 15 patients with tonsil hypertrophy and inflammation

as shown on schematic diagrams in Figure 1. Single-chain Fv form of an antibody was fused to truncated cp3 (scFv-cp3)³³ and expressed on the phage surface. Two types of antibody libraries were constructed and used in this study. One was scFv-cp3 consisting of V_H and V_L sequences recovered from lymphocytes in the tonsils which was designated as H1. The other was scFv-C_L-cp3 consisting of V_H and V_L-C_L sequences from the same sample and designated as H2 (Figure 1C). This study was approved by the Okayama University Ethics Committee and Medical & Biological Laboratories Co., Ltd Ethics Committee and was implemented according to the Ethical Guidelines for Human Genome/Gene Research enacted by the Japanese Government and the Helsinki Declaration.

2.3 | Screening of antihuman MSLN-scFv-cp3

Phages displaying scFv-cp3 which showed MSLN-binding activity were selected by a panning method. Recombinant soluble form (amino acids 297-580) of human MSLN (r-MSLN) was prepared according to Iwahori et al.³⁴ The phages recovered by the fourth or fifth round of panning with columns loaded with r-MSLN beads were infected into *Escherichia coli* and spread on a plate. Colonies were selected and grown in a liquid culture. Supernatants containing scFv-cp3 were used for screening by ELISA to evaluate specificity to MSLN. The 96-well microtiter plates were immobilized to the same r-MSLN. Epidermal growth factor receptor (EGFR) was used as a negative control. To select antihuman MSLN scFv-cp3s, rabbit anti-cp3 polyclonal antibody (Medical Biological Laboratories [MBL]) was used as the first antibody, and HRP-conjugated goat antirabbit IgG (H + L chain) was used as the second antibody. Finally, tetramethylbenzidine (TMB) was added and optical density (OD) was measured at 450 nm. Then the selected anti-MSLN scFv-cp3 were further selected by flow cytometry based on reactivity with cancer cell lines expressing MSLN on the cell surface (NCI-H226, NCI-N87 and BxPC-3). PANC-1 was used as an MSLN-negative cell line.

2.4 | Preparation of antihuman MSLN-scFv-His-Tag in mammalian cells

From the DNA sequence of a highly reactive scFv-cp3, we synthesized a scFv gene with a His-Tag sequence and expressed scFv using mammalian cells. Overall workflow for the preparation of humanized antihuman MSLN-scFv is shown in Figure 1C.

We synthesized an artificial gene of the V_H and V_L sequences of an anti-MSLN scFv-cp3 selected by ELISA and flow cytometry (FCM), and a linker and His-Tag were added to it. This gene was inserted into the mammalian cell expression vector pCx17.4 (Lonza) and genetically transfected into CHOK1-GSKO. Molecular sizes of the purified scFv preparations were estimated by SDS-PAGE. We also measured the molecular weight of the scFv with MALDI-time of flight mass spectrometry (MALDI-TOF-MS) (AXIMA Performance; Shimadzu).

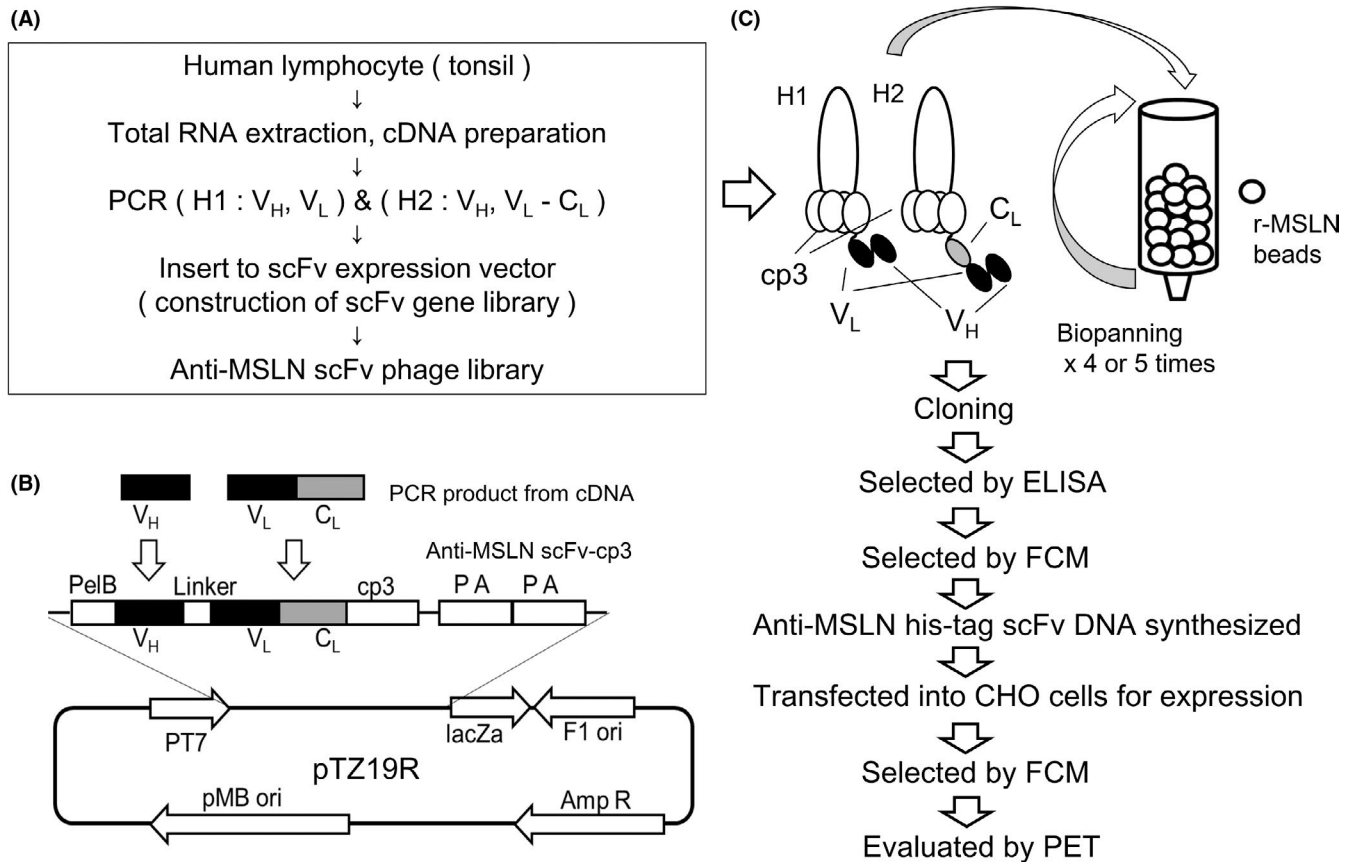


FIGURE 1 Schematic diagrams of the preparation and structure of the anti-mesothelin (MSLN) single-chain fragment of variable regions (scFv). A, Schematic diagram of the preparation of a naïve human scFv phage library using human tonsil lymphocytes. B, The scFv has a variable region of heavy and light chains and a structural linker with a cp3 sequence and a light chain constant region with PelB and cp3 sequences. PT7 has a T7 promoter. The variable region is shown in black, and the constant region is shown in gray. C, Schematic diagram of the preparation of an scFv with a His-Tag sequence and the concentration and selection of an scFv with a cp3 sequence (cp3-scFv). The cp3-scFv was concentrated by four to five rounds of bio-panning in a His-Tag column or mouse anti-His-Tag monoclonal antibody and Protein G column that uses beads to which human recombinant MSLN was bound. Individual cp3-scFv were cloned, and the binding ability to MSLN was evaluated by ELISA. scFv that were highly reactive according to ELISA were selected for their ability to bind to cancer cells, which was confirmed by flow cytometry (FCM). Based on the sequence information for selected scFv, we synthesized DNA of the scFv with a His-Tag sequence, expressed with Chinese hamster ovary (CHO) cells, and confirmed the ability to bind to cancer cells using FCM. scFv with a His-Tag sequence that was highly reactive based on FCM were evaluated by positron emission tomography (PET) imaging. V_H is the heavy chain variable region, V_L is the light chain variable region, and C_L is the light chain constant region. The variable region is shown in black, and the constant region is shown in gray

2.5 | Cell culture

Cancer cell lines established from various tissue types were purchased from ATCC and Japanese Collection of Research Bioresources (JCRB). Names of cell lines, tissue origins, and disease cases are shown in Table S1. All cells were cultured at 37°C in an incubator humidified with 5% CO₂.

2.6 | Flow cytometry analysis of antibodies

Human cancer cells (Table S1) were processed with enzyme-free cell dissociation buffer (Gibco/Life Technologies). Antihuman MSLN cp3-scFv, His-Tag scFv or full-length antihuman MSLN IgG were used for primary antibody. For antihuman MSLN cp3-scFv, we used antibody against *Protobothrops flavoviridis* venom hemorrhagic

factor HR1-007 as a negative control, and rabbit anti-cp3 polyclonal antibody (MBL) as a secondary antibody. For the tertiary antibody, Alexa Fluor 488-labeled goat antirabbit polyclonal antibody (Invitrogen) was used. For antihuman MSLN His-Tag scFv, as a secondary antibody, we used Alexa Fluor 488-labeled mouse anti-His-Tag mAb (MBL). As a control, we processed the cells without His-Tag scFv. Full-length antihuman MSLN or a negative control anti-KLH (IgG2b, isotype-matched) as the first antibody, and a goat polyclonal antimouse IgG labeled with Alexa Fluor 488 (Invitrogen) as a secondary antibody were used. Finally, the cells were suspended in PBS containing 7-AAD and EDTA for the exclusion of dead cells and examined with a BD FACSAria III flow cytometer (BD Biosciences). All antibodies were allowed to react for 1 hour on ice and, between the steps of the reaction, cells were washed twice. In addition, mean fluorescence intensity and exclusion of dead cells

were determined using BD FACSDiva software and calculated using Microsoft Excel.

2.7 | Deferoxamine-*p*-SCN conjugation and radiolabeling of His-Tag scFv

For DFO conjugation of His-Tag scFv, the ratio of dissolved chelating agent DFO (*p*-SCN-Bn-DFO) : His-Tag scFv was adjusted to a molar ratio of 3:1 and incubated for 1 hour in bicarbonate buffer (pH 9.0) at 37°C. ⁸⁹Zr was produced by a cyclotron (HM-12S; Sumitomo Heavy Industries, Ltd), purified from excess target material ⁸⁹Y, and obtained in 1 mol/L oxalic acid. ⁸⁹Zr-oxalate solution was neutralized by the addition of 2 mol/L Na₂CO₃, followed by 0.5 mol/L HEPES buffer (pH 7.0). The resultant ⁸⁹Zr solution was mixed with a DFO-modified His-Tag scFv clone in 0.9% sodium chloride/5 mg/mL gentisic acid (pH 5.0) and incubated at 37°C for 30 minutes to obtain ⁸⁹Zr-DFO-scFv. Unbound ⁸⁹Zr was removed through ultrafiltration using an Amicon Ultra 10K centrifugal filter and saline containing gentisic acid. Radiochemical purity was determined with TLC autoradiography (TLC-ARG) and HPLC (LC-20; Shimadzu) using a Superdex 200 10/300 column (GE Healthcare). Radioactivity was detected with a GABI Star detector (Raytest) connected to HPLC. In vitro stability of radiolabeled scFv after a 6-hour incubation in 50% human plasma/PBS at 37°C was also analyzed with HPLC. Furthermore, to evaluate changes in binding ability after DFO conjugation and ⁸⁹Zr marking, equilibrium dissociation constants (*K_D*) were measured with a BLItz intermolecular interaction analyzer (ForteBio, Inc.) with second-generation amine-reactive (ARG2) biosensor probes.

2.8 | Xenografts

All animal experiments were conducted in accordance with the guidelines of Okayama University and approved by the Institutional Animal Care and Use Committee (IACUC) at Okayama University (OKU-2013098). Five-week-old male BALB/c nu/nu mice were purchased from Charles River and were maintained under specific pathogen-free conditions at Department of Animal Resources, Advanced Science Research Center, Okayama University before use. For PET imaging, BALB/c nu/nu mice were grafted with NCI-N87 (3×10^6 cells) s.c. in the right shoulder as well as PANC-1 (1×10^7 cells) in the left shoulder. Imaging experiments were carried out when the tumor size reached approximately 8 mm in diameter.

2.9 | Positron emission tomography, computed tomography imaging and biodistribution of mice

Each mouse inoculated with NCI-N87 and PANC-1 cells was anesthetized by inhalation of isoflurane. ⁸⁹Zr-DFO-scFv was given into the tail vein of mice (*n* = 3), and a dynamic emission scan was acquired for 3 hours using a PET system (Clairvivo PET; Shimadzu). Mean amount of scFv given was 6.0 MBq/8.3 μg for H1a050 and 4.1 MBq/11.5 μg for H2a064. After the PET scan, computed tomography (CT) data

were obtained using a PET/CT system (Eminence Stargate; Shimadzu). Acquired PET data were reconstructed using 3-D-DRAMA. PET and CT images were converted to DICOM format and fused using PMOD software version 3.3 (PMOD Technologies Ltd). Three-dimensional volumes of interest (VOI) were manually drawn on PET/CT images to determine the mean percentage of the injected dose per gram of tissue (%ID/g) in heart as blood pool and tumors. After CT scanning, mice were dissected for biodistribution studies. Tumors and major organs were collected and weighed, and the radioactivity was measured with a gamma-counter (AccuFLEX γ7001; Hitachi Aloka Medical). Biodistribution data are expressed as %ID/g. Specificity of ⁸⁹Zr-DFO scFv H1a050 accumulation in NCI-N87 xenografts was tested by competition with excess amount of unlabeled scFv H1a050. NCI-N87 tumor-bearing mice (*n* = 6 mice /group) were injected with 1 μg (38 kBq) of ⁸⁹Zr-DFO scFv H1a050 with or without 49 μg unlabeled scFv H1a050. The mice were dissected at 3 hours after injection and the radioactivity of NCI-N87 xenograft was measured.

2.10 | Statistical analysis

Data are presented as the mean ± SD. Statistical analysis was carried out using a nonpaired Student's *t* test for comparison of two groups. Statistical significance was established at *P* < .05.

3 | RESULTS

3.1 | Construction of phage antibody library and screening of antihuman MSLN-scFv-cp3

From palatine tonsillar lymphocyte cDNA of patients with tonsil hypertrophy and inflammation, an antibody phage library was constructed. Through four to five rounds of bio-panning, 120 anti-MSLN cp3-scFv clones were obtained. Reactivity of the anti-MSLN cp3-scFv clones was examined in ELISA with solid-phase r-MSLN (Figure 2), allowing selection of 15 scFv clones with high reactivity to r-MSLN. The V_H sequence of each clone was confirmed (data not shown), and some clones had almost the same sequence. Among the homologous clones, the clones with the best specificity and reactivity to rMSLN were selected. For example, as H1a003, H1a005, H1a006, H1a012, H1a024, and H1a054 had the same sequence as H1a050, H1a050 was selected as a representative clone.

Reactivity of these anti-MSLN cp3-scFv clones was confirmed by FCM analysis. As target cells expressing MSLN, NCI-H226 (lung cancer cell line), NCI-N87 (gastric cancer cell line), and BxPC-3 (pancreatic cancer cell line) were used. As a negative control, pancreatic cancer cell line, PANC-1, which showed very weak expression of MSLN, was used. Through FCM analysis, we selected six scFv clones with high reactivity to MSLN-positive cancer cells and extremely weak or negative reactivity to PANC-1 (Figure 3). Some clones, such as H2a002, showed high reactivity in FCM but were excluded from selection as they showed nonspecific binding in ELISA. We found that there was a correlation between the ELISA and FCM data of cp3-scFv clones, which suggested that the anti-MSLN scFv clones prepared in

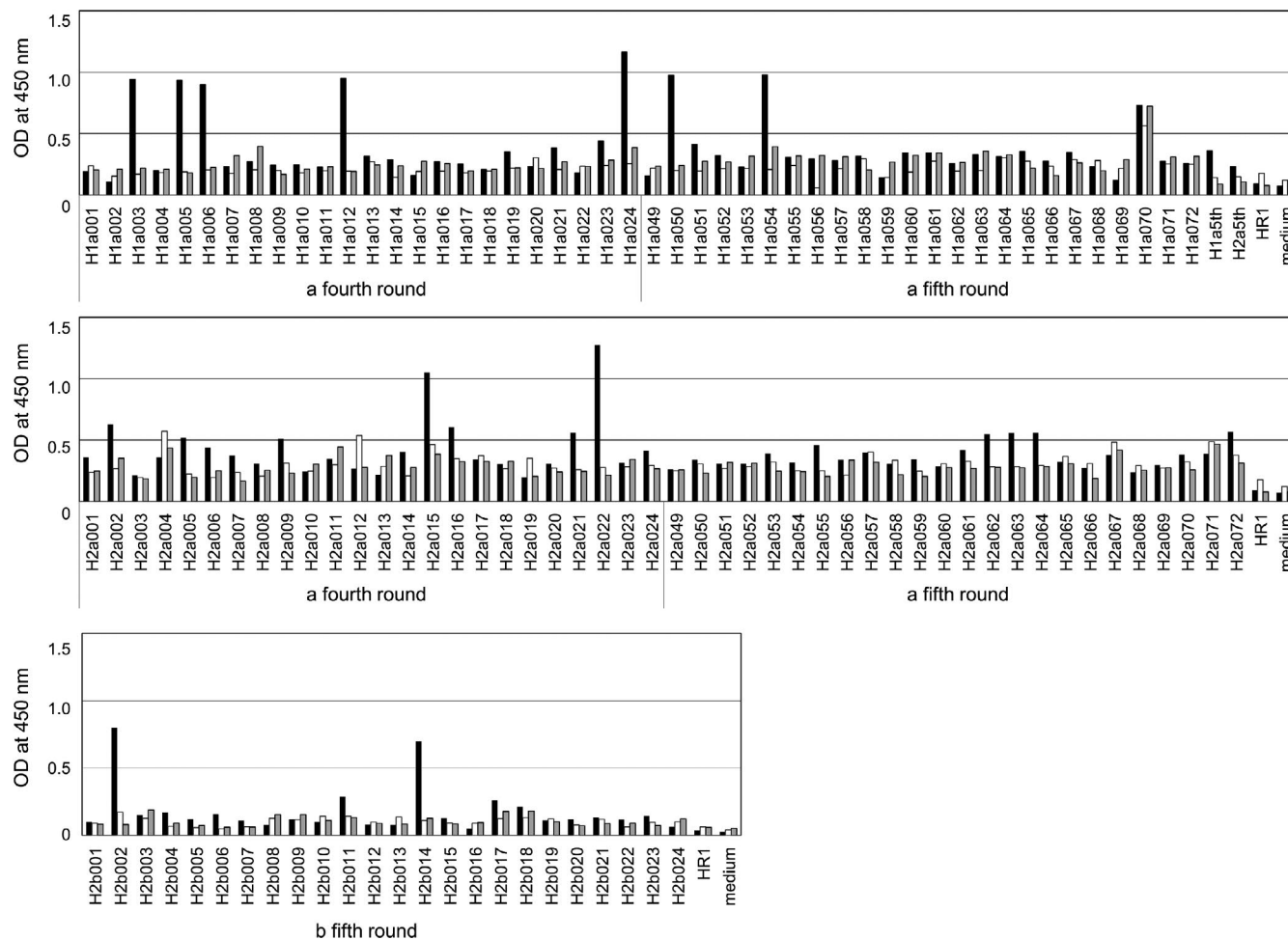


FIGURE 2 Single-chain fragment of variable regions (scFv) with a cp3 sequence (cp3-scFv) clone selection and evaluation by ELISA. Black bars indicate the reactivity of cp3- scFv against immobilized r-MSLN, gray bars indicate that against EGFR as a negative control, and white bars indicate that against PBS. HR1 is pc3-scFv specific for hub venom used as control. Each clone name is indicated on the X axis. (HR1 is control cp3-scFv. Medium is cell culture medium)

this study recognize the MSLN molecule on live cell membranes as well as the immobilized MSLN molecule on plastic plates (Figure S1).

3.2 | Preparation of antihuman MSLN-scFv-His-Tag in mammalian cells

In order to obtain structural authenticity and correct glycosylation pattern, scFv were generated by mammalian cells. Antihuman MSLN-scFv-His-Tag variants that can be produced in mammalian cells were prepared from the DNA sequences of the selected anti-MSLN cp3-scFv clones, inserted into a vector, and transfected into Chinese hamster ovary (CHO) cells (Figure 4A,B). We prepared six antihuman MSLN-scFv-His-Tag clones and carried out FCM analysis using each cancer cell line. Among them, clones H1a050 and H2a064 presented specific activity to MSLN-expressing cell lines. In particular, clone H1a050 showed high reactivity to MSLN expressed in cancers derived from various tissues (Figure 5). In addition, scFv H1a050 showed reactivity similar to that of full-length IgG anti-MSLN antibody 11-25 (Figure 5). FCM results of all six scFv clones with various cancer cell lines are shown in Figure S2. Structure of the

antihuman MSLN His-Tag-scFv and amino acid sequence of the six scFv clones are shown in Figure 4A,B, respectively.

Antihuman MSLN-scFv-His-Tag molecular weight estimated from DNA sequences was calculated to be 27 063.24 Da for H1a050 and 26 684.87 Da for H2a064. The approximate molecular weights of the six antihuman MSLN-scFv-His-Tag clones was confirmed by reduced SDS-PAGE (Figure 4C). The molecular weights determined by MALDI-TOF-MS were 26 926.58 Da for His-Tag scFv H1a050 and 26 547.88 Da for His-Tag scFv H2a064. Although there is a difference in molecular weight of approximately one amino acid residue, a peptide of nearly the estimated molecular weight was obtained.

3.3 | Deferoxamine-*p*-SCN conjugation and radiolabeling of His-Tag scFv

His-Tag scFv were modified with DFO and labeled with ^{89}Zr . Specific activity after ^{89}Zr labeling was 0.496 MBq/ μg and 0.365 MBq/ μg for H1a050 and H2a064, respectively. In vitro stability of ^{89}Zr -labeled scFv after 6-hour incubation in 50% human plasma at 37°C was

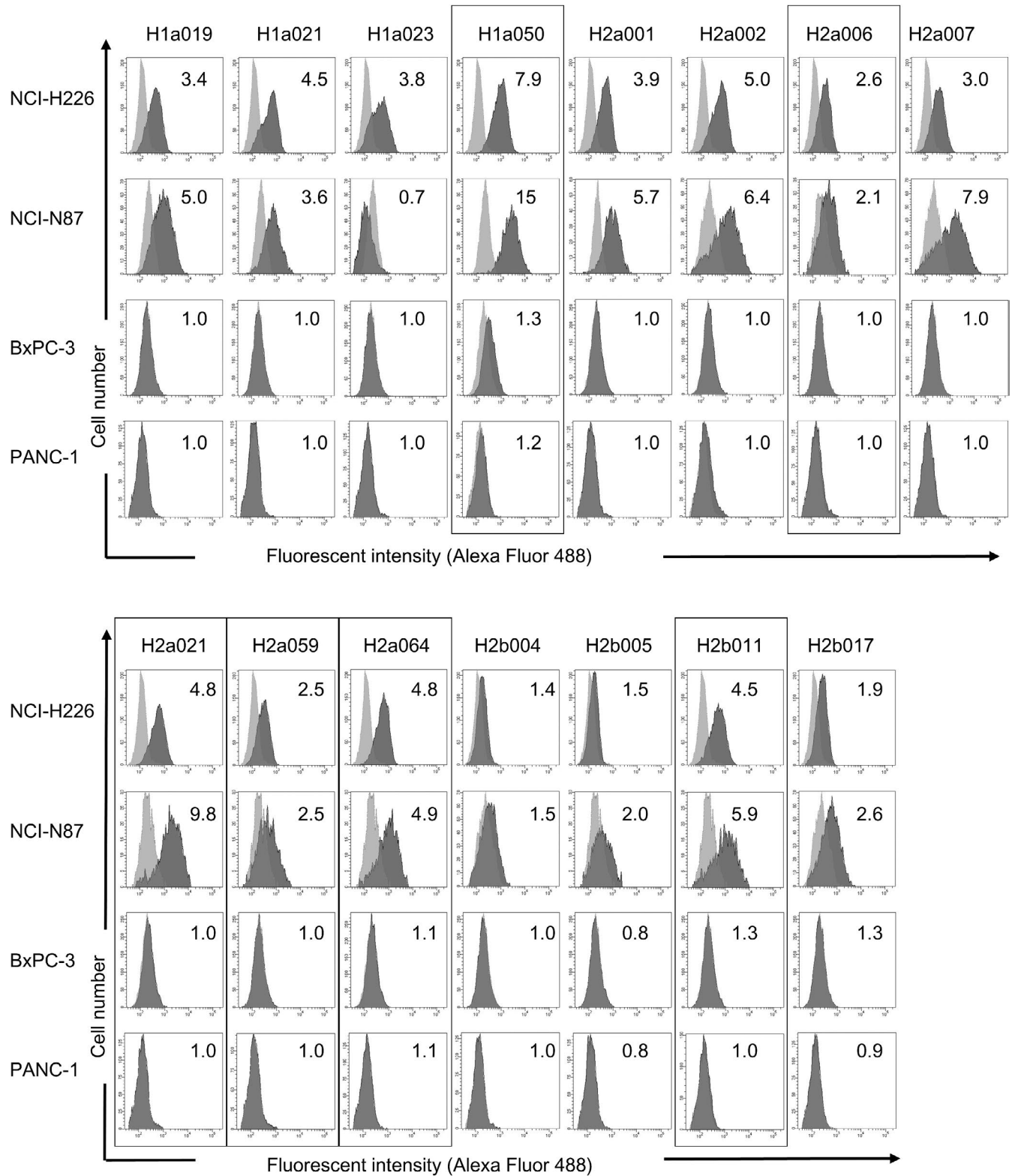


FIGURE 3 Evaluation of antihuman mesothelin (MSLN) single-chain fragment of variable regions (scFv) with a cp3 sequence (cp3-scFv) clones with flow cytometry (FCM). Using lung cancer cells (NCI-H226), gastric cancer cells (NCI-N87), pancreatic cancer cells (BxPC-3), and PANC-1, we analyzed the reactivity of antihuman MSLN cp3-scFv clones by FCM. Black indicates antihuman MSLN cp3-scFv clones, and gray shows the HR1-007 anti-*Protobothrops flavoviridis* venom scFv. Clones framed in black were selected for their high reactivity using FCM. Numbers indicate the ratio of the mean fluorescence intensity of each antihuman MSLN cp3-scFv clone to that of the HR1-007 anti-*P. flavoviridis* venom scFv used as a control

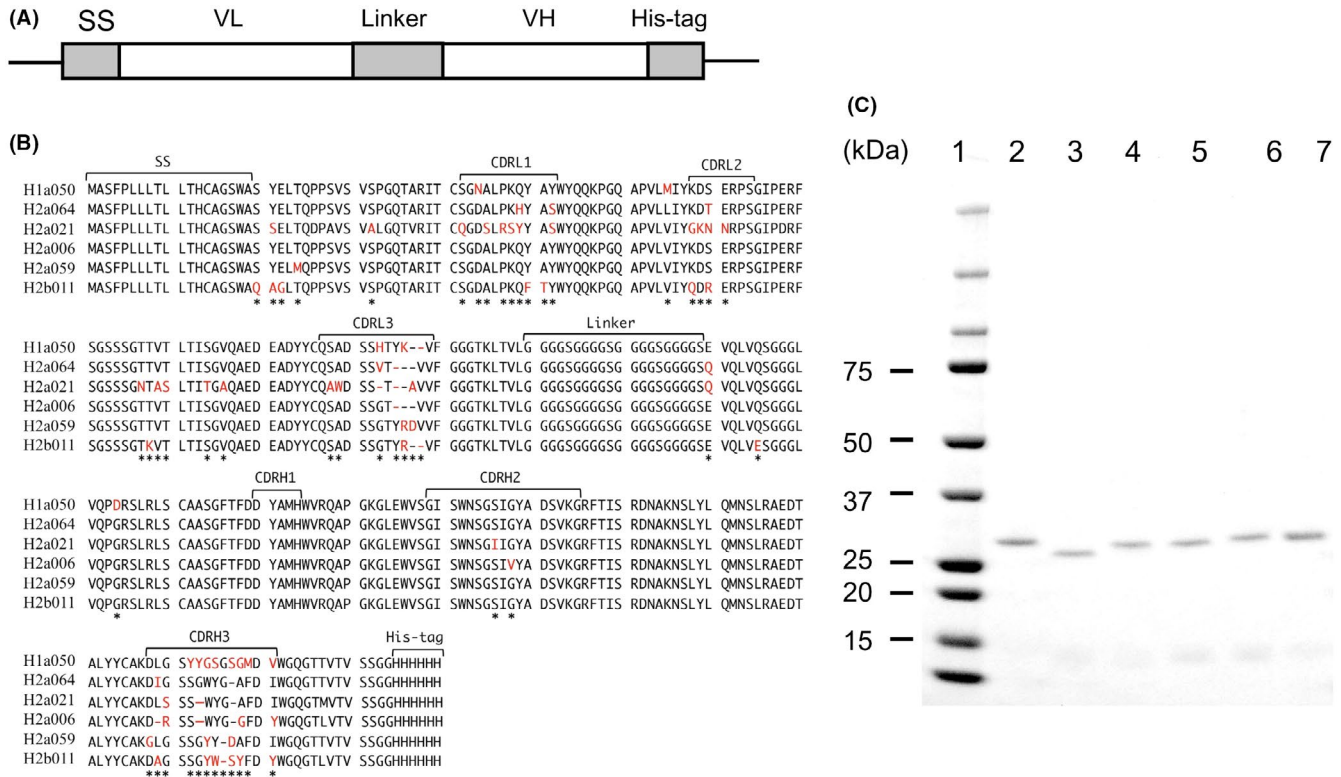


FIGURE 4 Structure of the obtained antihuman mesothelin (MSLN) His-Tag-single-chain fragment of variable regions (His-Tag scFv) and analysis by SDS-PAGE. A, Structure of the antihuman MSLN His-Tag scFv. V_L , light chain variable region. V_H , heavy chain variable region. SS, signal peptide sequence. B, Amino acid sequence of the antihuman MSLN His-Tag scFv. Complementarity determining regions (CDR) for V_L and V_H are shown in boxes. Each V_L and V_H region shows similarity within frames and clear differences in specific CDR. (*) indicates amino acid residues that are different between clones, and red letters show amino acid residues that are conserved in the CDR. The His-Tag consists of histidine with six residues. SS is a signal sequence. CDR were estimated based on V BASE (The MRC Centre for Protein Engineering, MRC Laboratory of Molecular Biology) data. C, Reduced SDS-PAGE analysis of the His-Tag scFv clone. Sample Reducing Agent contains 100 mmol/L DTT. 1, molecular size marker; 2, His-Tag scFv H1a050 (27 064.24 Da); 3, His-Tag scFv H2a064 (26 684.87 Da); 4, His-Tag scFv H2a021 (26 708.96 Da); 5, His-Tag scFv H2a006 (26 701.85 Da); 6, His-Tag scFv H2a059 (27 124.32 Da); 7, His-Tag scFv H2b011 (27 033.18 Da). The molecular weight was calculated based on the amino acid sequence

98.3% and 100%, for H1a050 and H2a064, respectively. In addition, the K_D of each scFv before DFO conjugation, after DFO conjugation, and after ^{89}Zr labeling were as follows: H1a050: 4.68×10^{-9} mol/L, 3.38×10^{-9} mol/L, and 4.62×10^{-8} mol/L; H2a064: 5.96×10^{-8} mol/L, 1.14×10^{-7} mol/L, and 7.82×10^{-8} mol/L.

3.4 | Positron emission tomography, CT imaging and biodistribution of mice

Figure 6A shows the representative PET and CT images at 3 hours after giving ^{89}Zr -labeled DFO-His-Tag scFv clones H1a050 and H2a064. Antihuman MSLN-scFv-His-Tag clone H1a050 showed higher accumulation in transplanted tumors from NCI-N87 compared with H2a064. Time-activity curve of ^{89}Zr -DFO-scFv clones in the blood (heart) showed rapid clearance with a half-life of approximately 15 minutes for H1a050 and 12 minutes for H2a064 (Figure 6B). ^{89}Zr -DFO-scFv H1a050 had the highest NCI-N87 tumor uptake (1.24%ID/g) approximately 4 minutes after injection, and the uptake decreased slowly and was retained at approximately 0.9%ID/g at 3 hours after administration (Figure 6C). Uptake of

^{89}Zr -DFO-scFv H1a050 of PANC-1 tumor was constantly lower than that of NCI-N87 tumor. ^{89}Zr -DFO-scFv H2a002 showed a similar uptake pattern for both NCI-N87 tumor and PANC-1 tumor, although their decline was faster than that of H1a050 (Figure 6D).

Figure 7A shows the biodistribution of ^{89}Zr -DFO-scFv H1a050 and H2a064 after 3 hours PET and CT imaging. ^{89}Zr -DFO-scFv H1a050 showed significantly higher accumulation in NCI-N87 tumors (1.54%ID/g) compared with that in PANC-1 tumors (0.78%ID/g) ($P < .05$). High accumulation of radioactivity was observed in the kidneys and liver, as they are major organs for scFv clearance.

Figure 7B shows the in vivo blocking experiment of ^{89}Zr -DFO-scFv H1a050. Tumor uptake of $1 \mu\text{g}$ of ^{89}Zr -DFO-scFv H1a050 was significantly blocked by excess amount of unlabeled scFv H1a050 molecules ($P < .005$), indicating the specificity of scFv H1a050 for MSLN-expressing cancer cells.

Mice bearing various sizes of NCI-N87 tumor underwent PET imaging with ^{89}Zr -labeled H1a050. NCI-N87 tumor was visualized by PET with ^{89}Zr -labeled H1a050 regardless of the size of the tumor (Figure 8A). Tumor uptake of scFv per weight was nearly consistent

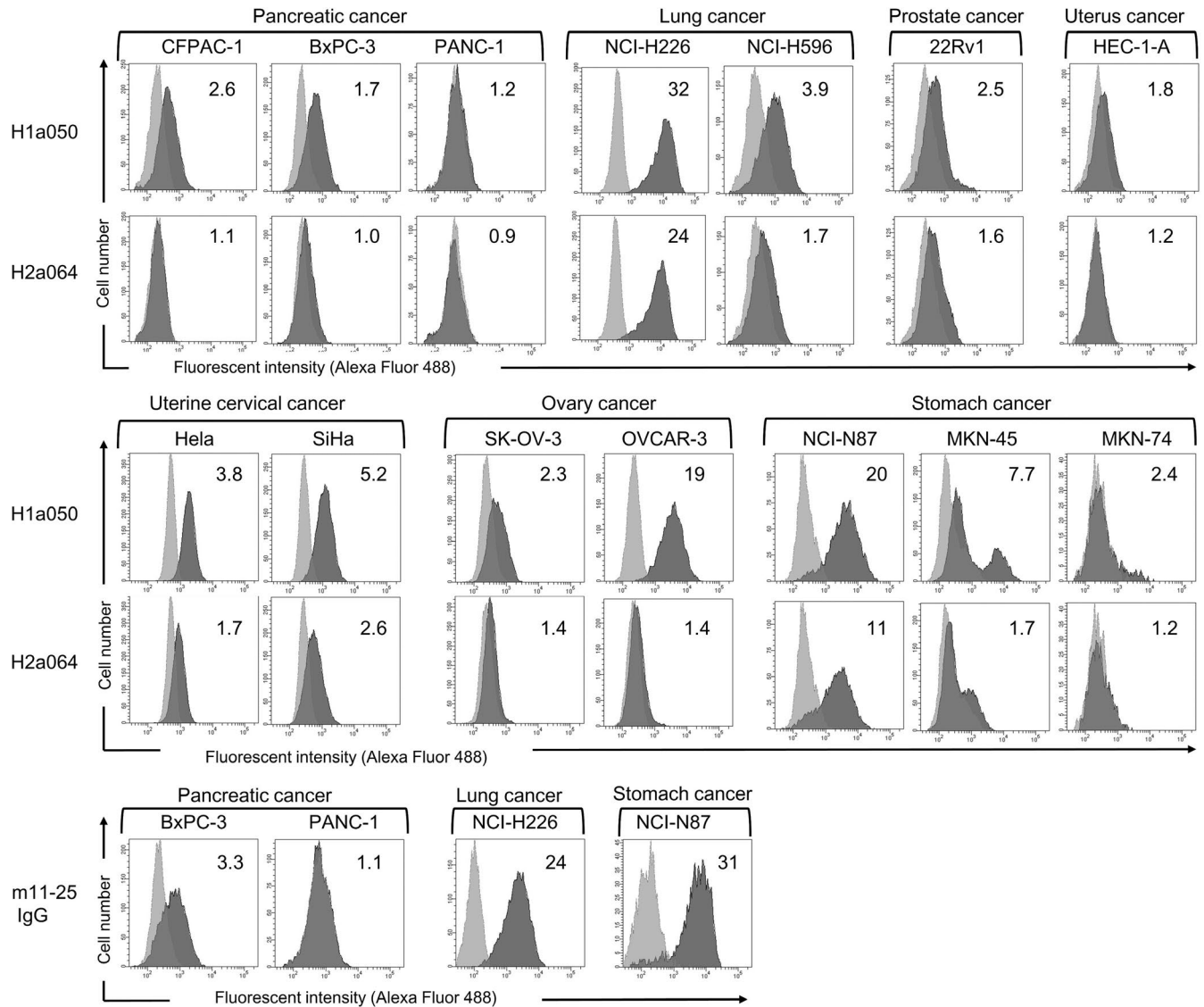


FIGURE 5 Evaluation of the antihuman His-Tag-single-chain fragment of variable regions (His-Tag scFv) clone in each cancer cell line. We analyzed the reactivity of the antihuman His-Tag scFv clone to three pancreatic cancer cell types, two lung cancer cell types, one type of prostate cancer cells, one uterine cancer cell type, two cervical cancer cell types, two ovarian cancer cell types, and three gastric cancer cell types by flow cytometry (FCM). Black indicates anti-human MSLN His-Tag scFv clone, gray indicates negative control. The negative control uses only the anti-His-Tag antibody as the secondary antibody without the anti-human MSLN His-Tag scFv clone as the primary antibody. Bottom row shows FCM results for the full-length mouse antihuman mesothelin (MSLN) antibody 11-25. Black indicates the full-length mouse antihuman MSLN antibody, and gray indicates the negative control, the IgG isotype control anti-KLH antibody. Values are the ratios of the mean fluorescence intensity (MFI) of each antihuman MSLN cp3-scFv and full-length mouse antihuman MSLN antibody 11-25 to the MFI of the control

(Figure 8B,D), so the uptake of scFv per tumor correlated with the size of the tumor (Figure 8C,E).

4 | DISCUSSION

In the present study, we prepared scFv against MSLN, a target molecule in cancers. We showed that MSLN-positive tumors in tumor-bearing mice could be visualized by PET imaging with ^{89}Zr -labeled anti-MSLN scFv (Figure 6). The scFv domains showed high

amino acid sequence identities, as well as the hypervariable region. Complementarity determining region (CDR) was rich in L1, L2, L3, and H3 changes. Meanwhile, H2 showed only slight differences in two amino acid residues, demonstrating extremely high homology. In addition, the "RPS" amino acid sequence of the CDRL2 domain and the "Q**DSS" amino acid sequence of the CDRL3 domain were conserved; thus, these amino acid residues strongly contributed to the antibody's affinity to human MSLN (Figure 4B).

Anti-MSLN cp3-scFv clones were selected by their reactivity in ELISA with r-MSLN and in FCM with cancer cell lines. Then the

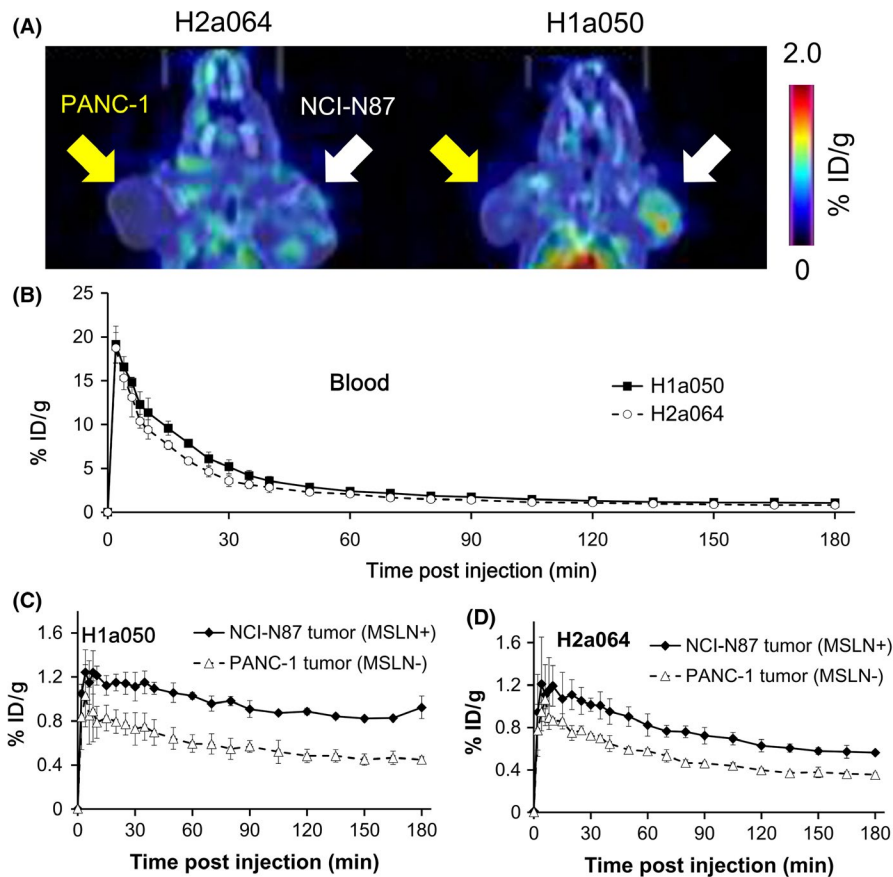


FIGURE 6 Positron emission tomography (PET) and computed tomography (CT) images obtained using the ^{89}Zr -deferoxamine-*p*-SCN-single-chain fragment of variable regions (^{89}Zr -DFO-scFv) that recognizes human mesothelin (MSLN) in a mouse model. Mice bearing tumors from gastric cancer cells showing high levels of MSLN expression (NCI-N87: right shoulder: white arrow) and pancreatic cancer cells with low levels of MSLN expression (PANC-1: left shoulder: yellow arrow). A, PET and CT images were obtained 3 h after giving ^{89}Zr -DFO-scFv that recognizes MSLN. H2a064 and H1a050 are the clone names for the antihuman His-Tag scFv. B-D, Graphs of temporal accumulation of ^{89}Zr -DFO-scFv in tumors and blood. B, Y-axis shows the accumulation of the antibody in blood. C, D, Y-axis shows the accumulation of the antibody in gastric cancer cells with high levels of MSLN expression (NCI-N87) and pancreatic cancer cells with low levels of MSLN expression (PANC-1), (%ID/g). Error bars indicate the SD

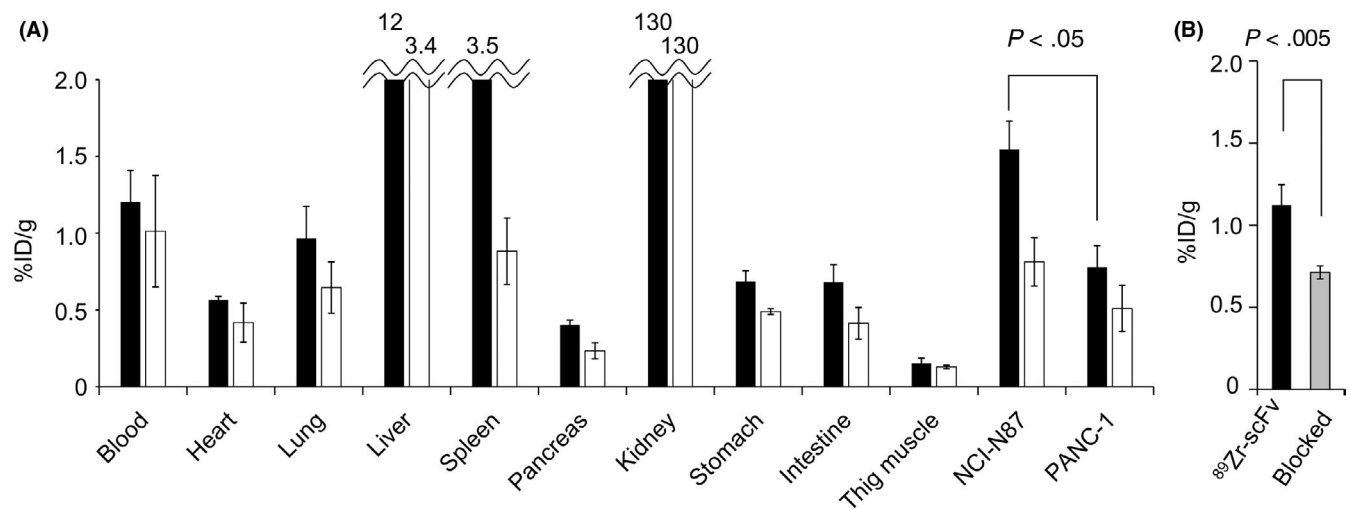


FIGURE 7 Biodistribution studies of ^{89}Zr -deferoxamine-*p*-SCN-single-chain fragment of variable regions (^{89}Zr -DFO-scFv). Biodistribution of ^{89}Zr -DFO-scFv at 3 h post-injection in tumor-bearing mice. Data were calculated as the % of injection dose per gram (%ID/g). A, Black bars indicate scFv H1a050; white bars indicate scFv H2a064. B, Blocking study using excess amount of unlabeled scFv. Black bar indicates tumor uptake 3 h after injection with 1 μg ^{89}Zr -labeled scFv; gray bar indicates that with 1 μg ^{89}Zr -labeled scFv with 49 μg unlabeled scFv. ($n = 6$, mean \pm SD)

selected scFv clones were produced in mammalian CHO cells. The reactivity of these clones was confirmed again using FCM, and two highly reactive scFv clones H1a050 and H2a064 were selected. These scFv clones showed specific reactivity to MSLN-expressing cancer cells derived from a wide range of tissues (Figure 5) with a

similar reactivity pattern to that of mouse antihuman MSLN full-length IgG antibody (Figure S1).

The selected scFv clones produced in CHO cells were modified with DFO and labeled with ^{89}Zr through DFO. According to the dissociation constant obtained by BLItz, radiolabeled scFv had sufficient

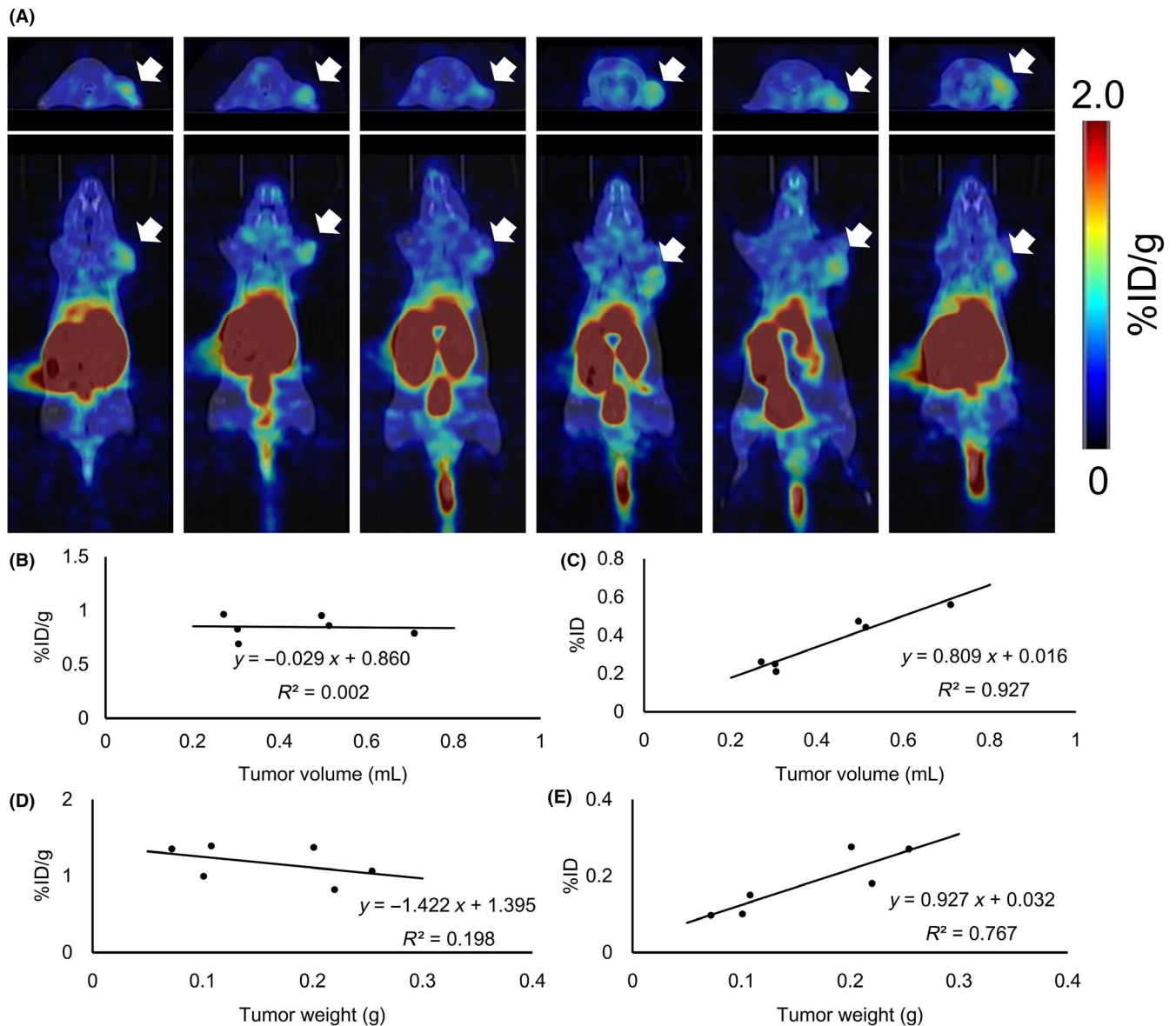


FIGURE 8 Positron emission tomography (PET) and computed tomography (CT) images of various sized tumor-bearing mice with ^{89}Zr -deferoxamine-*p*-SCN-single-chain fragment of variable regions (^{89}Zr -DFO-scFv) and correlation of tumor uptake of ^{89}Zr -DFO-scFv and tumor size. A, Axial and coronal PET/CT images of various sized tumor-bearing mice with ^{89}Zr -DFO-scFv (H1a050) at 3 h post-i.v. injection. Images are arranged in order of smaller tumor (left) to larger (right). White arrows indicate NCI-N87 tumors. B–E, Correlation of tumor uptake of ^{89}Zr -DFO-scFv and tumor size. Tumor uptake calculated by volumes of interest analyses of the PET data (B, C) and biodistribution study (D, E) are presented as %ID/g (B, D) and %ID (C, E)

antigen-binding activity. The radiolabeled scFv clones were also stable in 50% plasma at 37°C for 6 hours (98.3% and 100%). In PET imaging, ^{89}Zr -labeled scFv clearly showed the tumor derived from NCI-N87 cancer cells strongly expressing MSLN, but did not show the tumor by PANC-1 cells weakly expressing MSLN (Figure 6A).

As seen from the distribution in the blood and tumors, ^{89}Zr -labeled scFv was quickly discharged from the blood and retained in tumors even at 3 hours post-injection. The accumulation of NCI-N87 was almost twofold that of PANC-1 (Figure 6C). This indicates the potential of scFv H1a050 as a rapid PET probe for MSLN-positive cancer diagnosis. The mouse antihuman MSLN 11-25 IgG antibody we developed earlier was found to be useful for in vivo

near infrared fluorescence (NIRF) imaging, and ^{64}Cu PET imaging.³² However, for PET imaging with ^{64}Cu -DOTA-11-25 IgG, it took 24–48 hours after the administration to obtain images with fine contrast. This is likely an effect of recirculation of labeled antibody by the lymphatic system by recognition of the Fc domain through the embryonic Fc receptor and weak diffusion of the antibody from the vasculature because of its size.²⁹ Moreover, effects such as opsonization of the Fc domain inhibit specific examination of antibody molecules as probes. Therefore, in the present study, we imaged with scFv, which is a small molecule and a fragment without the Fc domain. scFv showed fast blood clearance, but tumor clearance is also reported to be fast.^{26–29} In vivo visualization with

scFv has been demonstrated with anti-tissue factor with a NIRF label.³⁵ However, with PET imaging, scFv is usually not used, and most imaging uses low molecular fragment antibody molecules such as scFv-Fc or diabody.^{36,37} The scFv prepared in the present study allowed visualization of tumors that express MSLN with PET at 3 hours after injection. As such, our antibodies would be useful for tumor imaging. There was a large amount of ⁸⁹Zr accumulation in the kidneys and liver as they are major organs for scFv clearance (Figure 7). Still, as there are reports of a method in which SMRP in blood is neutralized by giving unlabeled anti-MSLN antibody at the same time, and a method that regulates accumulation in the liver through chemical conjugation using Fab and ^{99m}Tc,³⁸ we may need to consider these methods to decrease ⁸⁹Zr accumulation in the liver.

A metallic positron emitter, ⁸⁹Zr, does not emit beta-minus particles. Therefore, radiation to the body can be controlled for greater safety. Moreover, because of its longer half-life (78.41 hours) compared to other PET nuclides, it can be used for various and more complex labeling and purification.³⁹

In conclusion, our novel anti-MSLN scFv specifically reacted with MSLN-positive cancer cells in vitro and could clearly visualize MSLN-positive tumors by in vivo PET imaging, which demonstrates its potential as an agent for imaging MSLN-positive cancer.

ACKNOWLEDGMENTS

This study was partly supported by a grant of the Japan Agency for Medical Research and Development, Project for Cancer Research and Therapeutic Evolution (P-DIRECT and P-CREATE).

DISCLOSURE

Authors declare no conflicts of interest for this article.

ORCID

Eiji Matsuura  <https://orcid.org/0000-0003-1681-0684>

REFERENCES

- Chang K, Pastan I. Molecular cloning of mesothelin, a differentiation antigen present on mesothelium, mesotheliomas, and ovarian cancers. *Proc Natl Acad Sci USA*. 1996;93:136-140.
- Hassan R, Bera T, Pastan I. Mesothelin: a new target for immunotherapy. *Clin Cancer Res*. 2004;10:3937-3942.
- Hassan R, Ho M. Mesothelin targeted cancer immunotherapy. *Eur J Cancer*. 2008;44:46-53.
- Argani P, Iacobuzio-Donahue C, Ryu B, et al. Mesothelin is overexpressed in the vast majority of ductal adenocarcinomas of the pancreas: identification of a new pancreatic cancer marker by serial analysis of gene expression (SAGE). *Clin Cancer Res*. 2001;7:3862-3868.
- Baba K, Ishigami S, Arigami T, et al. Mesothelin expression correlates with prolonged patient survival in gastric cancer. *J Surg Oncol*. 2012;105:195-199.
- Hassan R, Kreitman RJ, Pastan I, Willingham MC. Localization of mesothelin in epithelial ovarian cancer. *Appl Immunohistochem Mol Morphol*. 2005;13:243-247.
- Ordóñez NG. Application of mesothelin immunostaining in tumor diagnosis. *Am J Surg Pathol*. 2003;27:1418-1428.
- Ordóñez NG. Value of mesothelin immunostaining in the diagnosis of mesothelioma. *Mod Pathol*. 2003;16:192-197.
- Tchou J, Wang LC, Selven B, et al. Mesothelin, a novel immunotherapy target for triple negative breast cancer. *Breast Cancer Res Treat*. 2012;133:799-804.
- Dainty LA, Risinger JI, Morrison C, et al. Overexpression of folate binding protein and mesothelin are associated with uterine serous carcinoma. *Gynecol Oncol*. 2007;105:563-570.
- Steinbach D, Onda M, Voigt A, et al. Mesothelin, a possible target for immunotherapy, is expressed in primary AML cells. *Eur J Haematol*. 2007;79:281-286.
- Yu L, Feng M, Kim H, et al. Mesothelin as a potential therapeutic target in human cholangiocarcinoma. *J Cancer*. 2010;1:141-149.
- Chang K, Pastan I, Willingham MC. Isolation and characterization of a monoclonal antibody, K1, reactive with ovarian cancers and normal mesothelium. *Int J Cancer*. 1992;50:373-381.
- Scholler N, Fu N, Yang Y, et al. Soluble member(s) of the mesothelin/megakaryocyte potentiating factor family are detectable in sera from patients with ovarian carcinoma. *Proc Natl Acad Sci USA*. 1999;96:11531-11536.
- Beyer HL, Geschwindt RD, Glover CL, et al. MESOMARK: a potential test for malignant pleural mesothelioma. *Clin Chem*. 2007;53:666-672.
- Di Serio F, Fontana A, Loizzi M, et al. Mesothelin family proteins and diagnosis of mesothelioma: analytical evaluation of an automated immunoassay and preliminary clinical results. *Clin Chem Lab Med*. 2007;45:634-638.
- Pass HI, Wali A, Tang N, et al. Soluble mesothelin-related peptide level elevation in mesothelioma serum and pleural effusions. *Ann Thorac Surg*. 2008;85:265-272.
- Scherpereel A, Grigoriu B, Conti M, et al. Soluble mesothelin-related peptides in the diagnosis of malignant pleural mesothelioma. *Am J Respir Crit Care Med*. 2006;173:1155-1160.
- Grigoriu BD, Scherpereel A, Devos P, et al. Utility of osteopontin and serum mesothelin in malignant pleural mesothelioma diagnosis and prognosis assessment. *Clin Cancer Res*. 2007;13:2928-2935.
- Creaney J, van Bruggen I, Hof M, et al. Combined CA125 and mesothelin levels for the diagnosis of malignant mesothelioma. *Chest*. 2007;132:1239-1246.
- Cristaudo A, Foddìs R, Vivaldi A, et al. Clinical significance of serum mesothelin in patients with mesothelioma and lung cancer. *Clin Cancer Res*. 2007;13:5076-5081.
- Robinson BW, Creaney J, Lake R, et al. Soluble mesothelin-related protein—a blood test for mesothelioma. *Lung Cancer*. 2005;49:109-111.
- Goldenberg DM, Sharkey RM. Advances in cancer therapy with radiolabeled monoclonal antibodies. *Q J Nucl Med Mol Imaging*. 2006;50:248-264.
- Goldenberg DM, Sharkey RM. Novel radiolabeled antibody conjugates. *Oncogene*. 2007;26:3734-3744.
- McCardle RJ, Harper PV, Spar IL, Bale WF, Andros G, Jiminez F. Studies with iodine-131-labeled antibody to human fibrinogen for diagnosis and therapy of tumors. *J Nucl Med*. 1966;7:837-847.
- Colcher D, Pavlinkova G, Beresford G, Booth BJM, Choudhury A, Batra SK. Pharmacokinetics and biodistribution of genetically-engineered antibodies. *Q J Nucl Med*. 1998;42:225-241.
- Yokota T, Milenic DE, Whitlow M, Schlom J. Rapid tumor penetration of a single-chain Fv and comparison with other immunoglobulin forms. *Cancer Res*. 1992;52:3402-3408.
- Presta LG. Molecular engineering and design of therapeutic antibodies. *Curr Opin Immunol*. 2008;20:460-470.

29. Zalevsky J, Chamberlain AK, Horton HM, et al. Enhanced antibody half-life improves in vivo activity. *Nat Biotechnol.* 2010;28:157-159.
30. Skerra A, Plückthun A. Assembly of a functional immunoglobulin Fv fragment in *Escherichia coli*. *Science.* 1988;240:1038-1041.
31. Sai KS, Melinda W, Monica W, et al. Immuno-PET of epithelial ovarian cancer: harnessing the potential of CA125 for non-invasive imaging. *EJNMMI Res.* 2014;4:60.
32. Kobayashi K, Sasaki T, Takenaka F, et al. A novel PET imaging using ⁶⁴Cu-labeled monoclonal antibody against mesothelin commonly expressed on cancer cells. *J Immunol Res.* 2015;2015:268172.
33. McCafferty J, Griffiths AD, Winter G. Phage antibodies: filamentous phage displaying antibody variable domains. *Nature.* 1990;348:552-554.
34. Iwahori K, Osaki T, Serada S, et al. Megakaryocyte potentiating factor as a tumor marker of malignant pleural mesothelioma: evaluation in comparison with mesothelin. *Lung Cancer.* 2008;62:45-54.
35. Ryuta S, Toshifumi O, Ryo T, et al. Preparation and characterization of anti-tissue factor single-chain variable fragment antibody for cancer diagnosis. *Cancer Sci.* 2014;105:1631-1637.
36. Tove O, David B, Vania EK, et al. Recombinant anti-CD20 antibody fragments for microPET imaging of B-cell lymphoma. *J Nucl Med.* 2009;50:1500-1508.
37. Rochefort MM, Girgis MD, Knowles SM, et al. A mutated anti-CA19-9 scFv-Fc for positron emission tomography of human pancreatic cancer xenografts. *Mol Imaging Biol.* 2014;16:721-729.
38. Kim MK, Jeong HJ, Kao CH, et al. Improved renal clearance and tumor targeting of ^{99m}Tc-labeled anti-Tac monoclonal antibody Fab by chemical modifications. *Nucl Med Biol.* 2002;29:139-146.
39. Holland JP, Divilov V, Bander NH, Smith-Jones PM, Larson SM, Lewis JS. ⁸⁹Zr-DFO-J591 for immunoPET of prostate-specific membrane antigen expression in vivo. *J Nucl Med.* 2010;51:1293-1300.

SUPPORTING INFORMATION

Additional supporting information may be found online in the Supporting Information section at the end of the article.

How to cite this article: Yakushiji H, Kobayashi K, Takenaka F, et al. Novel single-chain variant of antibody against mesothelin established by phage library. *Cancer Sci.* 2019;110:2722-2733. <https://doi.org/10.1111/cas.14150>